Theoretical Studies of Inorganic and Organometallic Reaction Mechanisms. 18. Catalytic Transfer Dehydrogenation of Alkanes by an Iridium(III) Pincer Complex

Shuhua Li and Michael B. Hall*

Department of Chemistry, Texas A&M University, College Station, Texas 77843

Received January 26, 2001

Density functional theory has been used to investigate the mechanism of transfer dehydrogenation of ethane catalyzed by (PCP′)Ir(H)$_2$ [PCP′ = η^3-$C_6H_3(CH_2PH_2)_2$-1,3] with ethylene as the hydrogen acceptor. Our calculations show that the transfer dehydrogenation of ethane by (PCP′)Ir(H)$_2$ involves two stages: first, (PCP′)Ir(H)$_2$ is dehydrogenated by the hydrogen acceptor to produce the key intermediate (PCP′)Ir; second, ethane is dehydrogenated by (PCP′)Ir to produce the product ethylene and regenerate the catalyst (PCP′)Ir(H)$_2$. The three critical steps in this reaction are hydride transfer to ethylene, ethane oxidative addition, and dissociation of the coordinated ethylene, with barriers of 14.0, 11.6, and 23.4 kcal/mol, respectively. In contrast to acceptorless dehydrogenation catalyzed by the same pincer complex, where Ir(V) species are energetically accessible, here, the alternative path for transfer dehydrogenation involving Ir(V) intermediates is shown to be too endoergic.

Introduction

There have been extensive studies on alkane dehydrogenation by a variety of transition metal complexes in the past decades. Several catalytic systems were reported to dehydrogenate alkanes to alkenes thermochemically[1−13] or photochemically.[3,14] In the thermochemical cases, a sacrificial hydrogen acceptor is usually added to make the overall alkane dehydrogenation process thermodynamically favorable.[1−8] This type of dehydrogenation is often called transfer dehydrogenation because the hydrogens are transferred from the alkane to the hydrogen acceptor. Acceptorless thermochemical catalysts for alkane dehydrogenation are a recent development;[12,13] especially interesting is the high turnover rate for an Ir pincer complex recently reported by Liu and Goldman.[13] Clearly, a deeper understanding of the mechanism of alkane dehydrogenation by transition metal complexes is essential to design more efficient and more practical dehydrogenation catalysts.

Both experimental[3b,7,11d,15] and theoretical studies[16,17] have been carried out to explore the mechanisms of alkane dehydrogenation by iridium and rhodium complexes. It is generally accepted[3,15,17] that alkane dehydrogenation reactions involve the following consecutive steps: (i) oxidative addition of the substrate alkane, (ii) ligand rearrangement, dissociation, or a reductive elimination, to create a vacant site for the formation of the β-agostic intermediate, (iii) β-H transfer from the alkyl ligand to the metal, and (iv) loss of the coordinated olefin. The rate-determining step could be any one of the above four steps and could depend on the catalyst.

Recently, the iridium(III) complexes (PCP)Ir(H)$_2$ [PCP = η^3-$C_6H_3(CH_2PR_2)_2$-1,3 (R=Bu^t,Pr^i)] were found to be highly efficient thermochemical catalysts for acceptorless dehydrogenation at about 200 °C[12,13] and transfer

---

[1] Crabtree, R. H.; Mihelcic, J. M.; Quirk, J. M. *J. Am. Chem. Soc.* **1979**, *101*, 7738.

[2] Baudry, D.; Ephritikhine, M.; Felkin, H.; Holmes-Smith, R. *J. Chem. Soc., Chem. Commun.* **1983**, 788.

[3] (a) Burk, M. W.; Crabtree, R. H.; McGrath, D. V. *J. Chem. Soc., Chem. Commun.* **1985**, 1829. (b) Burk, M. W.; Crabtree, R. H. *J. Am. Chem. Soc.* **1987**, *109*, 8025. (c) Burk, M. W.; Crabtree, R. H.; Parnell, C. P.; Uriarte, R. J. *Organometallics* **1984**, *3*, 816.

[4] (a) Felkin, H.; Fillebeen-Khan, T.; Holmes-Smith, R.; Zakrzewski, V. G. *Tetrahedron Lett.* **1984**, *25*, 1279. (b) Felkin, H.; Fillebeen-Khan, T.; Holmes-Smith, R.; Lin, Y. *Tetrahedron Lett.* **1985**, *26*, 1999.

[5] (a) Maguire, J. A.; Goldman, A. S. *J. Am. Chem. Soc.* **1991**, *113*, 6706. (b) Maguire, J. A.; Petrillo, A.; Goldman, A. S. *J. Am. Chem. Soc.* **1992**, *114*, 9492.

[6] Miller, J. A.; Knox, L. K. *J. Chem. Soc., Chem. Commun.* **1994**, 1449.

[7] Belli, J.; Jensen, C. M. *Organometallics* **1996**, *15*, 1532.

[8] Braustein, P.; Chauvin, Y.; Nahring, J.; Decian, A.; Fischer, J.; Tiripicchio, A.; Ugozzoli, F. *Organometallics* **1996**, *15*, 5551.

[9] (a) Fujii, T.; Satio, Y. *J. Chem. Soc., Chem. Commun.* **1990**, 757. (b) Fujii, T.; Higashino, Y.; Satio, Y. *J. Chem. Soc., Dalton Trans.* **1993**, 517.

[10] Aoki, T.; Crabtree, R. H. *Organometallics* **1993**, *12*, 294.

[11] (a) Gupta, M.; Hagen, C.; Flesher, R. J.; Kaska, W. C.; Jensen, C. M. *Chem. Commun.* **1996**, 2083. (b) Gupta, M.; Hagen, C.; Kaska, W. C.; Cramer, R. E.; Jensen, C. M. *J. Am. Chem. Soc.* **1997**, *119*, 840. (c) Gupta, M.; Kaska, W. C.; Jensen, C. M. *Chem. Commun.* **1997**, 461. (d) Lee, D. W.; Kaska, W. C.; Jensen, C. M. *Organometallics* **1998**, *17*, 1. (e) Jensen, C. M. *Chem. Commun.* **1999**, 2443.

[12] Xu, W.-W.; Rosini, G. P.; Gupta, M.; Jensen, C. M.; Kaska, W. C.; Krough-Jespersen, K.; Goldman, A. S. *Chem. Commun.* **1997**, 2273.

[13] Liu, F.; Goldman, A. S. *Chem. Commun.* **1999**, 655.

[14] (a) Nomura, K.; Saito, Y. *J. Chem. Soc., Chem. Commun.* **1988**, 161. (b) Nomura, K.; Saito, Y. *J. Mol. Catal.* **1989**, *54*, 57. (c) Sakakura, T.; Sodeyama, T.; Tanaka, M. *New J. Chem.* **1989**, *13*, 737. (d) Maguire, J. A.; Boese, W. T.; Goldman, A. S. *J. Am. Chem. Soc.* **1989**, *111*, 7088. (e) Sakakura, T.; Sodeyama, T.; Abe, F.; Tanaka, M. *Chem. Lett.* **1991**, 297.

[15] Van der Boom, M. E.; Higgitt, C. L.; Milstein, D. *Organometallics* **1999**, *18*, 2413.

[16] (a) Strout, D.; Zaric, S.; Niu, S.-Q.; Hall, M. B. *J. Am. Chem. Soc.* **1996**, *118*, 6068. (b) Su, M.-D.; Chu, S.-Y. *J. Am. Chem. Soc.* **1997**, *119*, 5373. (c) Niu, S.-Q.; Hall, M. B. *J. Am. Chem. Soc.* **1998**, *120*, 6169. (d) Han, Y.-Z.; Deng, L.-Q.; Ziegler, T. *J. Am. Chem. Soc.* **1997**, *119*, 5939.

[17] Niu, S.-Q.; Hall, M. B. *J. Am. Chem. Soc.* **1999**, *121*, 3992.

10.1021/om010065q CCC: $20.00
Publication on Web 05/02/2001

Scheme 1

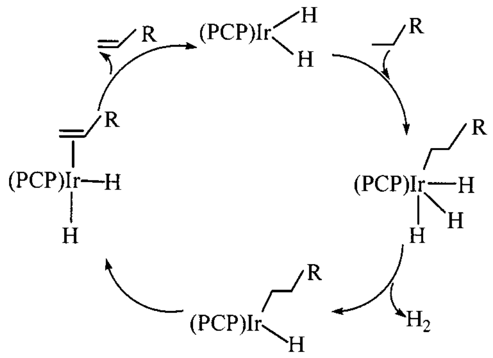

dehydrogenation at temperatures as low as 100 °C.[11a] Since the reaction conditions under which (PCP)Ir$(H)_2$ dehydrogenates alkanes to alkenes with and without the use of a hydrogen acceptor differ significantly from each other, the catalytic cycle under these two circumstances could be different; that is, different transition states and intermediates could be involved. The mechanism of alkane acceptorless dehydrogenation has been theoretically elucidated by Niu and Hall[17] by using density functional theory (DFT)[18] to study the model system (PCP′)Ir$(H)_2$ [PCP′ = η^3-$C_6H_3(CH_2PH_2)_2$-1,3] plus ethane. Their calculations showed a catalytic cycle (Scheme 1) consisting of three crucial steps: ethane oxidative addition, dihydride reductive elimination, and loss of the coordinated ethylene. Because the calculated barriers for these three steps are 16, 15, and 22 kcal/mol, respectively, the reaction's large overall endothermicity can be achieved in stages. These results convincingly explain why (PCP)Ir$(H)_2$ catalyzes the acceptorless dehydrogenation of alkanes;[12,13] a higher temperature is needed in the acceptorless case to overcome the large endothermicity of the overall reaction.

However, the mechanistic details of alkane transfer dehydrogenation by (PCP)Ir$(H)_2$ are not yet well understood. On the basis of the mechanism for acceptorless dehydrogenation,[17] one might suggest the mechanism displayed in Scheme 2. The lower cycle of this scheme is exactly the same as that given in Scheme 1, and the upper cycle is the reverse, as it represents the hydrogen transfer to the alkene. An alternative mechanism has been suggested by Jensen (Scheme 3).[11e] In this mechanism, the C−H activating intermediate is the 14-electron (PCP)Ir complex, not the 16-electron (PCP)Ir$(H)_2$ complex as in acceptorless dehydrogenation. In addition to the above two pathways, a third possible reaction pathway is shown in Scheme 4. Here, an alkyl hydride complex, generated from the partial dehydrogenation of (PCP)Ir$(H)_2$ by the hydrogen acceptor, could be the key intermediate that activates the C−H bond of the alkane.

Using density functional theory, we will investigate the possible mechanisms for transfer dehydrogenation by this iridium pincer complex. Together with our previous results[17] on acceptorless dehydrogenation, this work will provide a complete picture of the mechanism of the dehydrogenation of alkanes by the catalyst (PCP)Ir$(H)_2$. To reduce the size of systems studied, we chose (PCP′)Ir$(H)_2$ as a model for (PCP)Ir$(H)_2$ and used ethane and ethylene as models of a typical alkane and a hydrogen acceptor, respectively.

Scheme 2

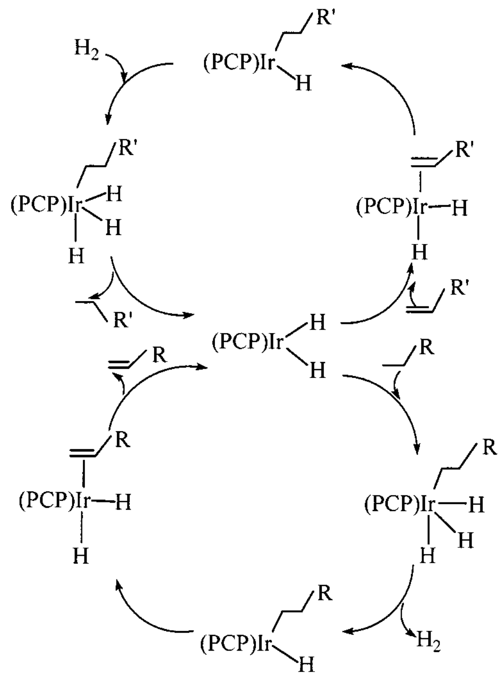

Scheme 3

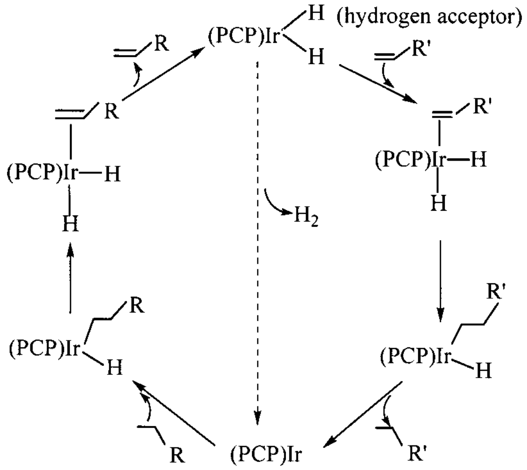

Computational Details

All the calculations have been performed with the Gaussian 94[19] package. Density functional theory was employed with the three-parameter hybrid exchange functional of Becke[20] and the Lee, Yang, and Parr correlation functional[21] (B3LYP). Relativistic effective core potentials (ECPs)[22] for iridium and

---

(18) Frisch, M. J.; Trucks, G. W.; Schlegel, H. B.; Gill, P. M. W.; Johnson, B. G.; Robb, M. A.; Cheeseman, J. R.; Keith, T.; Petersson, G. A.; Montgomery, J. A.; Raghavachari, K.; Al-Laham, M. A.; Zakrzewski, V. G.; Ortiz, J. V.; Foresman, J. B.; Peng, C. Y.; Ayala, P. Y.; Chen, W.; Wong, M. W.; Andres, J. L.; Replogle, E. S.; Gomperts, R.; Martin, R. L.; Fox, D. J.; Binkley, J. S.; Defrees, D. J.; Baker, J.; Stewart, J. P.; Head-Gordon, M.; Gonzalez, C.; Pople, J. A. *Gaussian 94*, Revision B.3; Gaussian Inc.: Pittsburgh, PA, 1994.

(19) Parr, R. G.; Yang, W. *Density-functional theory of atoms and molecules*; Oxford University Press: Oxford, 1989.

(20) (a) Becke, A. D. *Phys. Rev.* **1988**, *A38*, 3098. (b) Becke, A. D. *J. Chem. Phys.* **1993**, *98*, 1372. (c) Becke, A. D. *J. Chem. Phys.* **1993**, *98*, 5648.

(21) Lee, C.; Yang, W.; Parr, R. G. *Phys. Rev.* **1988**, *B37*, 785.

(22) (a) Hay, P. J.; Wadt, W. R. *J. Chem. Phys.* **1985**, *82*, 299. (b) Wadt, W. R.; Hay, P. J. *J. Chem. Phys.* **1985**, *82*, 284.

Scheme 4

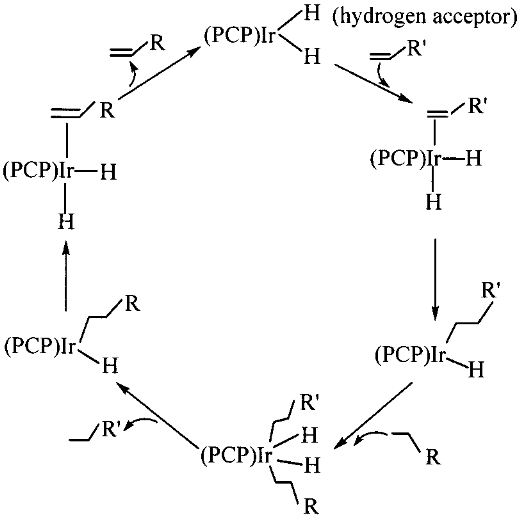

phosphorus were employed in all B3LYP calculations. In the ECP for Ir, the 5s and 5p orbitals were treated explicitly along with the 5d, 6s, and 6p valence orbitals. The basis set for Ir was a double-ζ basis set (341/541/21), where the two outermost 6p functions of the standard LANL2DZ[23] have been replaced by a (41) split of the optimized 6p function from Couty and Hall.[24] For P, the standard LANL2DZ basis set was augmented by a d-type polarization function.[25] The carbon and hydrogen atoms were described by the 6-31G(d,p) basis set[26] except for the uncoordinated carbons and hydrogens in the PCP′ ligand, where a 3-21G basis set[27] was used.

All intermediates and transition states (TS) were obtained by full geometry optimizations at the B3LYP level. The transition states, checked by separate frequency calculations, have only one imaginary frequency. Because frequencies were not calculated for all species, zero-point energy corrections were not performed. The addition of these corrections would not change our conclusions. The basis-set superposition error (BSSE) corrections[28] were included in calculating the association energies of ethane and ethylene with the iridium complexes.

Results and Discussion

As mentioned above, transfer dehydrogenation proceeds at a much lower temperature than acceptorless dehydrogenation. Because Scheme 2 consists of two independent cycles which are highly endoergic and exoergic, respectively, low-temperature transfer dehydrogenation is unlikely by this route. Schemes 3 and 4 represent mechanisms that avoid the highly endoergic cycle of Scheme 2. Thus, we will begin by examining Scheme 3, where the first stage in the catalytic cycle produces the key intermediate (PCP)Ir from (PCP)Ir$(H)_2$ either by the direct reductive elimination of H_2 or by dehydrogenation with the hydrogen acceptor. In the second stage, the alkane is dehydrogenated by (PCP)Ir to produce the product alkene and regenerate the catalyst (PCP)Ir$(H)_2$. With ethylene as the hydrogen acceptor and ethane as the reactant, the dehydrogenation of (PCP′)Ir$(H)_2$ by the hydrogen acceptor is obviously a reversal of the second stage, ethane dehydrogenation by (PCP′)Ir. Therefore, for Scheme 3, we begin with an exploration of the potential energy profile of the second stage, e.g., ethane dehydrogenation by the key intermediate (PCP′)Ir. Scheme 4, which involves the oxidative addition of ethane to the alkyl hydride complex forming an Ir(V) rather than the Ir(I) intermediate, will be explored later in this section.

Ethane Dehydrogenation by (PCP′)Ir. Ethane dehydrogenation may proceed along two different pathways (a and b in Figure 1). From the position of ethylene with respect to the PCP′ ligand before dissociation, a and b are referred to as the cis- and trans-pathways, respectively. First, we describe the mechanisms (Figure 1) and energetics (Table 1) of these two pathways, then the structural details (Figure 2) of the key species.

Cis-Pathway. From (PCP′)Ir (**1**), ethane dehydrogenation starts with the formation of the α-agostic complex **2**. Then, one C−H bond of ethane oxidatively adds to the metal with a barrier of 11.6 kcal/mol to generate the alkyl hydride intermediate **4**. Following the cis-pathway (Figure 1a), **4** isomerizes to another alkyl hydride complex **6** through the transition state **5** with an activation barrier of only 0.7 kcal/mol. By rotating the ethyl group, **6** readily converts into the β-agostic complex **8** through the transition state **7** with a barrier of 4.6 kcal/mol. The β-H transfer from the β-agostic alkyl group to the metal in **8** to form the alkene cis-dihydride complex **10** is exoergic by 10.6 kcal/mol with an activation barrier of 3.4 kcal/mol. Although we searched for the transition state for the dissociation of ethylene from **10**, we have not been able to find one. By performing several restrained optimizations described in a later section, we will show that the barrier for dissociation of ethylene should be approximately 23.4 kcal/mol (without BSSE correction). Since the binding energy of ethylene with the cis-dihydride complex **11** is 22.2 kcal/mol (without BSSE correction), the barrier for the reverse reaction, the attachment of ethylene by the cis-dihydride, can be estimated to be small. Thus, the BSSE-corrected dissociation energy for ethylene (18.8 kcal/mol) should be close to the actual barrier. Clearly, the loss of ethylene from the ethylene hydride complex **10** is the rate-determining step in the cis-pathway.

Trans-Pathway. As an alternative, after reaching **4**, ethane dehydrogenation may proceed along the trans-pathway. The ethyl ligand in **4** readily rotates through the transition state **12** to form another alkyl hydride complex **13**, which is 1.4 kcal/mol lower in energy than **4** and 1.1 kcal/mol lower in energy than its cis analogue, **6**. As the methyl group of the ethyl ligand in **13** rotates, the β-agostic alkyl hydride intermediate **15** forms with a barrier of only 2.4 kcal/mol. **15** is 1.4 kcal/mol more stable than its cis analogue **8**. The β-H transfer from **15** to yield the alkene hydride complex **17** through the transition state **16** is exoergic by 9.4 kcal/mol with a barrier of 5.5 kcal/mol. Finally, as described in a later section, our restrained optimizations show that the elimination of ethylene from **17** must directly produce the trans-dihydride **18** without a barrier beyond its endoergicity, which requires 27.8 kcal/mol, 9.0 kcal/mol

---

[23] LANL2DZ: Dunning D95 basis sets on first row, Los Alamos ECP plus double-ζ basis sets on Na−Bi.

[24] Couty, M.; Hall, M. B. *J. Comput. Chem.* **1996**, *17*, 1359.

[25] Höllwarth, A.; Böhme, M.; Dapprich, S.; Ehlers, A. W.; Gobbi, A.; Jonas, V.; Köhler, K. F.; Stegmann, R.; Veldkamp, A.; Frenking, G. *Chem. Phys. Lett.* **1993**, *208*, 237.

[26] Harihan, P. C.; Pople, J. A. *Theor. Chim. Acta* **1973**, *28*, 213.

[27] Hehre, W. J.; Radom, L.; Schleyer, P. v. R.; Pople, J. A. *Ab initio molecular orbital theory*; Wiley: New York, 1986.

[28] Boys, S. F.; Bernardi, F. *Mol. Phys.* **1970**, *19*, 553.

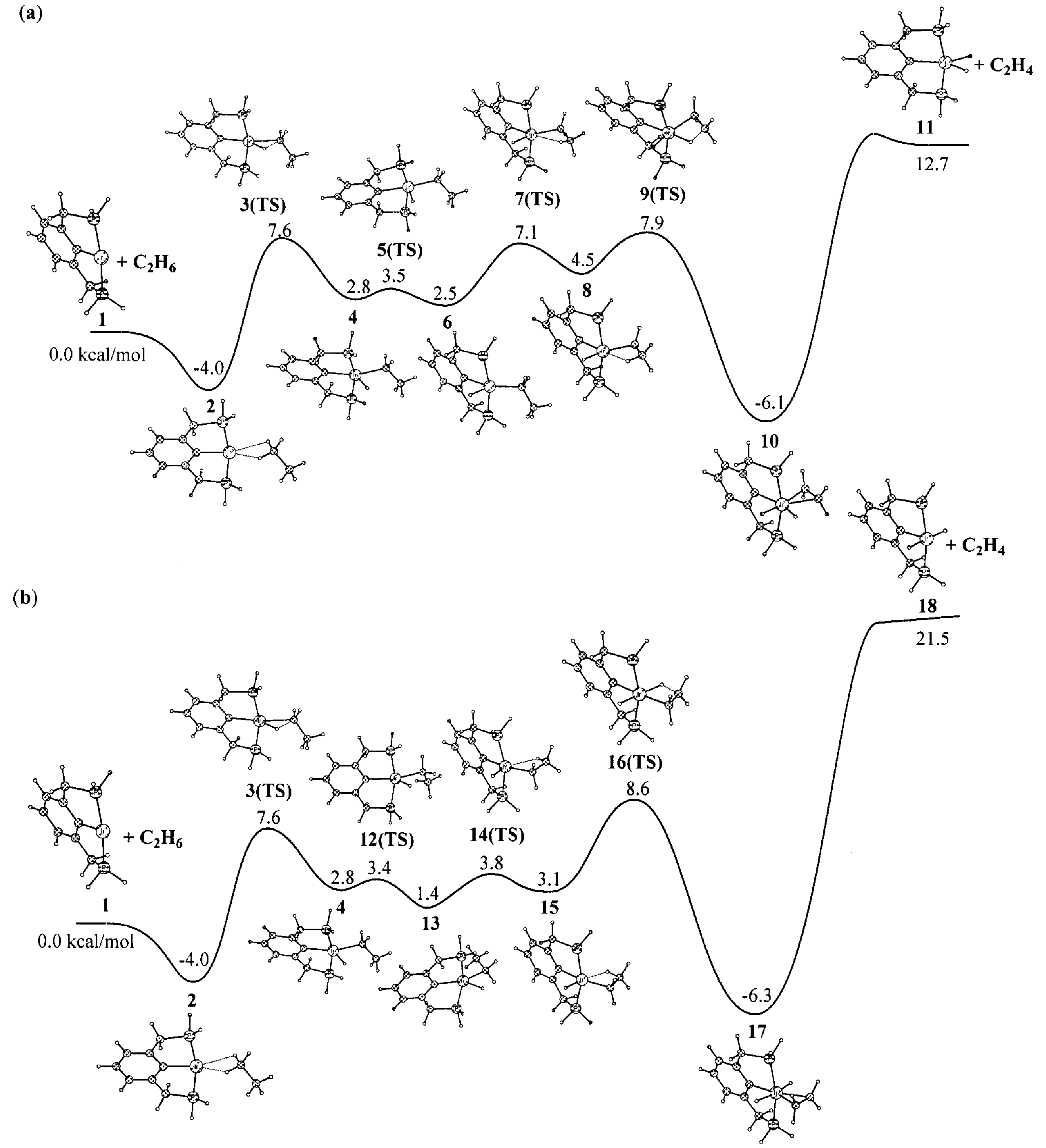

Figure 1. Potential energy profiles for ethane dehydrogenation by (PCP′)Ir. The upper (a) and lower (b) curves correspond to the cis- and trans-pathways, respectively.

more than that needed from **10** to **11** + C_2H_4. Then, the trans-dihydride complex **18** could convert to its cis-dihydride isomer **11**, which is 8.8 kcal/mol more stable than **18**, with an activation barrier of only 0.4 kcal/mol.[17]

Overall Cycle. By comparing the energetics of the above two pathways (Table 1), one finds that the cis-pathway is favored over the trans-pathway because the elimination of ethylene in the former is much more facile than it is in the latter. Although the completion of the reaction along the trans-pathway is blocked at **17**, species such as **13**, **15**, and **17** may still occur during the catalytic cycle because they are thermodynamically and kinetically accessible. Summarizing the above discussions, we can see that ethane oxidative addition and the loss of the coordinated ethylene, with barriers of 11.6 and 18.8 kcal/mol, are two critical steps for ethane dehydrogenation by (PCP′)Ir. Now, formation of this critical intermediate, (PCP′)Ir, could occur by the reverse of the half-cycle shown in Figure 1a or by direct H_2 reductive elimination. In the reverse half-cycle the largest barrier step is hydride transfer to olefin, **10** → **8**, which via transition state **7** has a barrier of 14.0 kcal/mol. Our calculations for the direct elimination of H_2 from (PCP′)Ir(H)$_2$ show this reaction to be endoergic by

Table 1. Relative Electronic Energies Δ*E* (kcal/mol)[a]

species	Δ*E*	species	Δ*E*
1 + C_2H_6	0.0	**10**	−6.14
2	−4.01	**11** + C_2H_4	12.73 (16.10)[b]
3(TS)	7.62	**12**(TS)	3.44
4	2.80	**13**	1.38
5(TS)	3.46	**14**(TS)	3.83
6	2.48	**15**	3.15
7(TS)	7.08	**16**(TS)	8.62
8	4.54	**17**	−6.26
9(TS)	7.88	**18** + C_2H_4	21.50 (24.35)[b]

[a] See the numbering of species in Figure 2. The transition states are explicitly denoted as (TS). [b] With and (without) basis set superposition error corrections.

26.0 kcal/mol. Thus, the formation of the critical 14-electron intermediate takes place by hydride transfer to olefin.

Geometries Along the Cis-Pathway. Geometric details are shown in Figure 2. The 14-electron intermediate **1**, (PCP′)Ir, has a T-shaped geometry, as expected for a d^8 ML_3 complex.[29] According to our calculations, **1** has a singlet ground state, with the lowest triplet state 25.8 kcal/mol above the ground state.

The intermediate **2** is a typical α-agostic complex. Although there are two close Ir−H contacts, one C−H bond interacts more strongly with the Ir atom than the other, as shown by their corresponding Ir−H bond distances of 2.017 and 2.554 Å, respectively. The hypothetical agostic complex with two identical Ir−H bond lengths is not a minimum, but a transition state. In comparison to free ethane, the two interacting C−H bonds in **2** are 0.036 and 0.001 Å longer. Relative to the reactant **1**, the Ir−C(PCP′) bond lengthens by 0.029 Å, a result of the weak trans effect of the α-agostically bound ethane.

The oxidative addition transition state **3** and the resulting alkyl hydride intermediate **4** are distorted trigonal bipyramids. Clearly, **3** is a late transition state because the C−H bond breaking and the Ir−H and Ir−C bond formation are nearly complete in **3**. The opening of the H−Ir−C^α angle from 43.7° to 70.9° is primarily responsible for the stabilization energy (about 4.8 kcal/mol) of **4** over **3**.

The intermediate **6** is a trigonal bipyramid with the hydride close to the PCP′ ligand. The transition state **5** between **4** and **6** is a square pyramid with the hydride trans to the vacant site. The intermediate **8** has a β-agostic alkyl ligand with the agostic C^β−H bond trans to the PCP′ ligand. The β-agostic interaction is quite strong in **8**, as evidenced by the relatively short distance (1.985 Å) between Ir and the β-H. However, **8** is 2.0 kcal/mol higher in energy than **6** because of two destabilizing factors. One is the torsional strain resulting from the eclipsed conformation of the ethyl ligand; the other is the angle strain due to the much smaller Ir−C^α−C^β angle (81.8°) than that in a normal metal alkyl (120.5° as in **6**). The transition state **7** between **6** and **8** has a very weak β-agostic interaction with the Ir−H interaction at 2.568 Å.

The alkene dihydride intermediate **10** adopts a pseudooctahedral structure. The C═C bond distance in **10** is 1.407 Å, 0.077 Å longer than that calculated for free ethylene. The β−H transfer transition state **9** is a four-centered transition state. Although one would expect **9** to be an early transition state, the C^β−H bond length of 1.491 Å in **9** implies that the C^β−H bond breaking is almost complete. Likewise, the Ir−H bond making is nearly complete in **9** because the Ir−H bond distance of 1.719 Å is very close to the corresponding value, 1.638 Å, in the β−H transfer product **10**. In contrast, the C^α−C^β bond distance in **9** is 1.453 Å, halfway between the 1.518 Å distance in **8** and the 1.407 Å distance in **10**, which means that the C^α−C^β bond formation is halfway toward the product **10**. The final product, cis-dihydride **11**, is a distorted trigonal bipyramid with a small H−Ir−H angle.

Geometries Along the Trans-Pathway. Although the trans-pathway is not likely to be involved in the complete cycle, several species on this path are fairly stable. Therefore, we will briefly discuss the structures for these species. The cis- and trans-pathways are identical until **4**, where the shift of the hydride ligand produces **6** on the cis-pathway and the rotation of the ethyl ligand produces **13** on the trans-pathway. The transition state **14** has a weak β-agostic interaction with an Ir−H distance of 2.431 Å. The β-agostic alkyl hydride intermediate **15** differs from its counterpart **8** on the cis-pathway mainly in that the interacting C^β−H bond is cis to the PCP′ group. The alkene dihydride intermediate **17** resembles **10** except that the alkene ligand now is trans to the PCP′ ligand. Apart from these structural differences, **15**, **16**, and **17** bear a strong resemblance to **8**, **9**, and **10**, respectively. The final product **18**, generated by the loss of ethylene from **17**, is a square pyramid with two hydrides trans to each other. The Ir−H distance in **18** is 0.084 Å longer than that in **11**, a reflection of the strong trans influence of the hydride ligand.

Ethylene Dissociation. Because automatic procedures failed to find a transition state for the dissociation of ethylene from **17** and **10**, we searched the potential energy curves for ethylene dissociation from these two molecules by performing several restrained optimizations along the approximate dissociation coordinate $R_{\mathrm{Ir-ethylene}}$ for each molecule.[30] From the results shown in Figure 3, one can see that as the Ir−ethylene distance increases, the calculated energy along the cis-pathway (with respect to the energy of the alkene complex **10**) increases monotonically. When $R_{\mathrm{Ir-ethylene}}$ is 4.5 Å, the optimized C═C bond length of the ethylene unit is 1.331 Å in the cis-pathway, being very close to the optimized distance of free ethylene (1.330 Å). At this point, the calculated energy in the cis-pathway is 23.4 kcal/mol higher than that of the alkene complex **10**. This result clearly shows that the barrier for the dissociation of ethylene from **10** should be approximately 23.4 kcal/mol (without BSSE corrections and along an approximate dissociation coordinate $R_{\mathrm{Ir-ethylene}}$). Furthermore, because DFT methods are not particularly accurate for van der Waals interactions, a weakly bound precursor

---

(29) Albright, T. A.; Burdett, J. K.; Whangbo, M. H. *Orbital interaction in chemistry*; Wiley: New York, 1985.

(30) For ethylene dissociation from **17** and **10**, the two Ir−C (ethylene) bond lengths are assumed to be identical along the reaction coordinate. This assumption should work well for **17** since the two Ir−C (ethylene) bonds are equal in **17**. However, because the two Ir−C (ethylene) bonds are not equal in **10**, the energy calculated by assuming two identical Ir−C bonds should provide an upper bound to the corresponding value along the “true” ethylene dissociation coordinate.

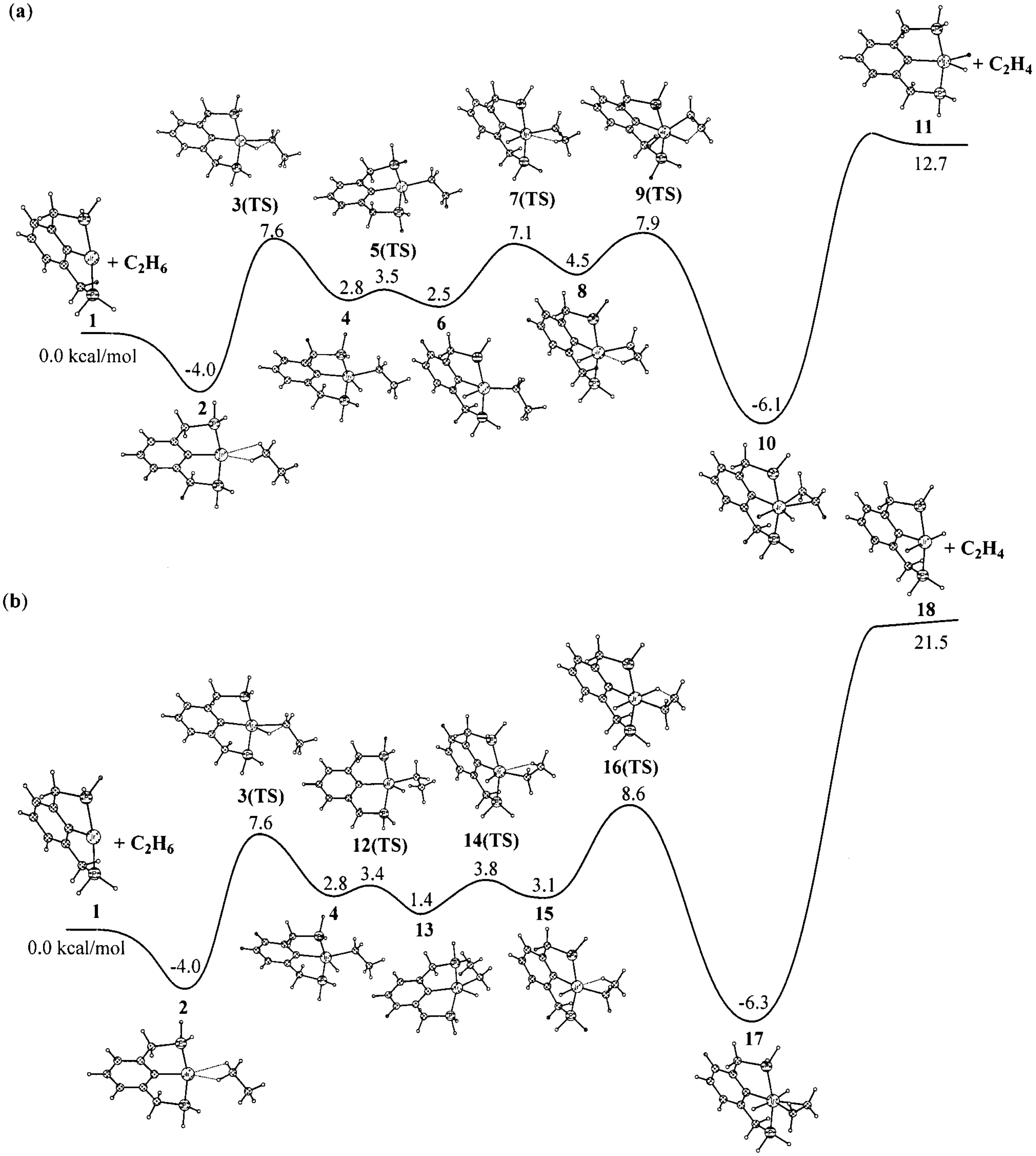

Figure 2. B3LYP-optimized structures of the reactant, intermediates, transition states, and products along the two pathways in Figure 1.

complex might not be detected by his approach. Is summary, these results suggest that there is essentially no barrier to the recombination of ethylene with **11** or **18** and that the ethylene dissociation barrier should be close to the BSSE-corrected dissociation energy.

On the other hand, we notice that the increase of energy is always larger along the trans-pathway than that along the cis-pathway. Since the barrier for conversion from the trans dihydride **18** to the cis dihydride **11** is only 0.4 kcal/mol,[17] one might wonder if the trans-pathway can easily cross over to the cis-pathway as the Ir−ethylene bond is gradually stretched. When $R_{\text{Ir-ethylene}}$ is stretched to 3.2 Å in the trans-pathway, the calculated energy cost is already 22.0 kcal/mol, close to that of the dissociation limit of ethylene along the cis-pathway. By checking the optimized geometry at this point (even $R_{\text{Ir-ethylene}} = 3.5$ Å), we find that the two hydrides keep their positions virtually unchanged from those of the equilibrium structure **17**. Therefore, the conversion from **18** to **11**, which has been studied previously,[31] must occur after the ethylene dissociation is nearly complete. In summary, our restrained optimizations suggest that

---

[31] Riehl, J. F.; Jean, Y.; Eisenstein, O.; Pelissier, M. *Organometallics* **1992**, *11*, 729.

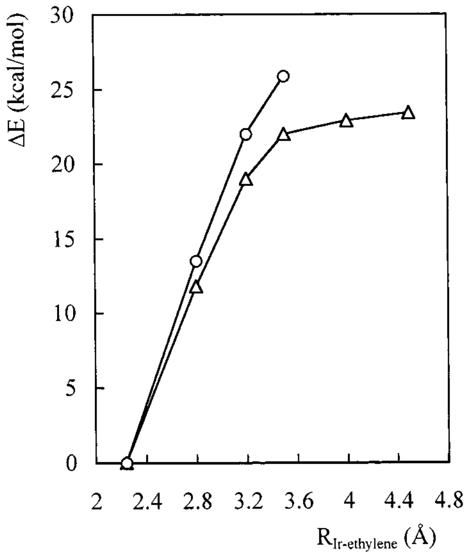

Figure 3. Electronic-energy change along approximate ethylene dissociation coordinate $R_{\text{Ir-ethylene}}$ relative to the energies of **10** and **17**. △ and ○ symbolize the cis- and trans-pathways, respectively.

the elimination of ethylene is more facile along the cis-pathway than along the trans-pathway.

Ethane Oxidative Addition by the Alkyl Hydride Complex. As an alternative to the cycle discussed above, Scheme 4 shows a cycle involving an Ir(V) intermediate. The optimized structures along this pathway are collected in Figure 4. Ethane activation begins with the formation of the agostic intermediate **19**, which is only 0.3 kcal/mol higher in energy than **4** plus ethane. Then, ethane oxidatively adds to the metal to generate two Ir(V) products, **20** and **21**, which are 16.4 and 20.5 kcal/mol above **19**, respectively. In comparison with the oxidative addition of ethane to **1**, as shown in Figure 1, the oxidative addition of ethane to the alkyl hydride complex, **4**, is less favorable because the barrier for ethane oxidative addition by **4** must be more than 16.4 kcal/mol, a value that is already 4.8 kcal/mol higher than the corresponding barrier for **1**.

In addition, the agostic intermediate **19** could also convert into **23** by reductively eliminating the alkyl and hydride ligands through the transition state **22**, with ethane acting as a solvent. The geometries of **22** and **23** are also shown in Figure 4. Structurally, **22** and **23** may be considered to be **3** and **2** loosely "solvated" by an ethane, respectively. Energetically, **23** is 6.7 kcal/mol more stable than **19**. The calculated reductive elimination barrier, 4.8 kcal/mol, is identical to the calculated barrier from **4** to **2** (see Figure 1) without the association of ethane to the metal. Thus, our calculations suggest that the association of ethane has little influence on the potential energy surface of the reductive elimination process of the alkyl and hydride ligands from the intermediate **4**.

On the basis of these results, we conclude that ethane oxidative addition is unlikely to occur at the 16-electron Ir(III) intermediate **4**. However, the "solvated" species such as **19** and **23** could form during the catalytic cycle because they are thermodynamically and kinetically accessible.

Proposed Mechanism. As discussed above, the mechanism shown in Scheme 4 can be excluded as the favored mechanism for the catalytic transfer dehydro-

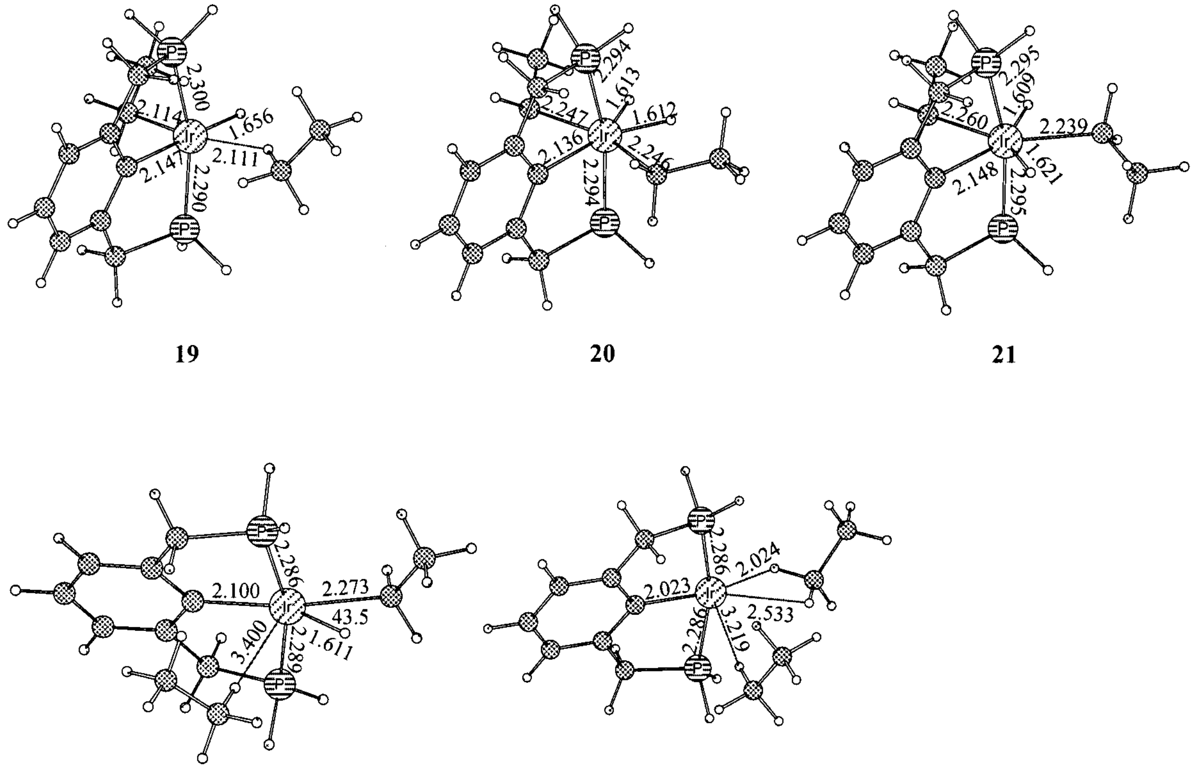

19 **20** **21**

22(TS) **23**

Figure 4. B3LYP-optimized structures of species involved in the oxidative addition of ethane to the alkyl hydride intermediate **4**.

Scheme 5

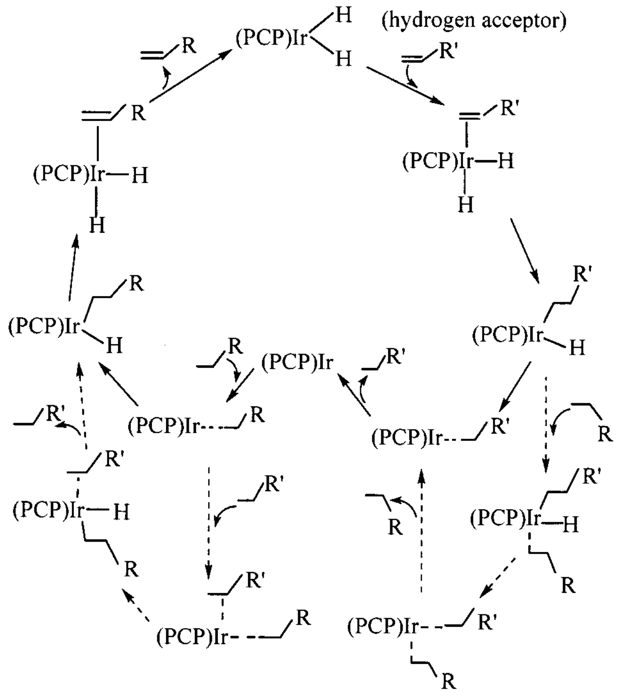

genation of ethane by (PCP′)Ir(H)$_2$. By comparing our previous results[17] for Scheme 2 and the present results for Scheme 3, we find that Scheme 3 represents the most likely mechanism. Although the largest barrier in these two schemes is the same, e.g., the elimination of ethylene, two additional barriers of 15 and 16 kcal/mol are crossed in the lower cycle of Scheme 2, whereas only one additional barrier of 11.6 kcal/mol is crossed in the half-cycle (ethane dehydrogenation) of Scheme 3. In addition, the high endothermicity of one of the half-cycles of Scheme 2 suggests that transfer dehydrogenation along the pathway of Scheme 2 would be slow at lower temperatures. Our calculations also show that a solvent could play a role in the dehydrogenation process of (PCP′)Ir(H)$_2$ by the hydrogen acceptor to produce the active intermediate (PCP′)Ir. We modeled this solvation by using an additional ethane molecule as a “solvent” molecule. However, these structures should only be taken as representative structures for solvation or intramolecular agostic interactions. By including those agostic structures and “solvated” species, our final proposed mechanism is shown in Scheme 5.

Conclusions

Density functional theory has been used to investigate the mechanism of ethane transfer dehydrogenation catalyzed by (PCP′)Ir(H)$_2$ in the presence of ethylene as the hydrogen acceptor. Our calculations show that the transfer dehydrogenation of ethane by (PCP′)Ir(H)$_2$ involves two stages: first, (PCP′)Ir(H)$_2$ is dehydrogenated by the hydrogen acceptor to produce the 14-electron intermediate (PCP′)Ir; second, ethane is dehydrogenated by (PCP′)Ir to produce the product ethylene and regenerate the catalyst (PCP′)Ir(H)$_2$. The half-reaction, ethane dehydrogenation by (PCP′)Ir, was calculated to be endoergic by 12.7 kcal/mol and proceeds by a cis-pathway, where the final product ethylene dissociates from the position cis to the (PCP′) ligand. For the whole catalytic cycle, three critical steps are hydride transfer to ethylene, ethane oxidative addition, and dissociation of the coordinated ethylene, with barriers of 14.0, 11.6, and 23.4 kcal/mol, respectively. Although the calculations show that species solvated by ethane (or by other solvents) or intramolecular agostic interactions could occur in the catalytic cycle, their presence has little impact on the potential energy surface.

In contrast to acceptorless dehydrogenation by (PCP′)Ir(H)$_2$ in which the C−H activating species is the 16-electron (PCP′)Ir(H)$_2$ complex, the most active intermediate for activating the C−H bond of ethane in transfer dehydrogenation is the 14-electron complex (PCP′)Ir. Whereas the acceptorless catalytic cycle involves Ir(III) and Ir(V) species, the transfer catalytic cycle proceeds via Ir(I) and Ir(III) species. Our mechanism proposed for the transfer dehydrogenation of ethane by (PCP′)Ir(H)$_2$ is consistent with the experimental reaction conditions in which the real catalyst (PCP)Ir(H)$_2$ dehydrogenates alkanes to alkenes with the use of a hydrogen acceptor at temperatures as low as 100 °C.[11a] Thus, it is expected that this mechanism should apply to the catalytic transfer dehydrogenation of alkanes by the real catalyst (PCP)Ir(H)$_2$.

Acknowledgment. We would like to thank National Science Foundation (Grant No. CHE 9800184) and The Welch Foundation (Grant No. A-648) for their generous support.

OM010065Q